

# Reduction of Input Torque and Joint Reactions in High-Speed Mechanical Systems with Reciprocating Motion

VIGEN ARAKELIAN<sup>1,2</sup>

<sup>1</sup>LS2N-ECN UMR 6004, 1 rue de la Noë,  
BP 92101, F-44321 Nantes,  
FRANCE

<sup>2</sup>MECAPROCE / INSA-Rennes,  
20 av. des Buttes de Coesmes,  
CS 70839, F-35708 Rennes,  
FRANCE

*Abstract:* - In high-speed machinery, the variable inertia forces generated by reciprocating masses often introduce undesirable effects, such as a significant increase in the required input torque and joint forces. This paper addresses the challenge of reducing input torque and joint reaction forces in such mechanisms by employing two compression linear springs positioned between the slider and the frame. These springs counterbalance the slider's inertia force, thereby diminishing both the input torque and joint reactions. It is important to note that the elastic forces exerted by these springs remain internal to the mechanical system, preserving the balance of shaking forces and moments of the mechanism on the frame. The analytical framework developed in this study focuses on minimizing the root mean square and maximum values of the inertia force effects. A significant scientific achievement is attaining a given goal through an analytical solution. Notably, this is the first instance where this problem has been formulated and solved using explicit expressions. The effectiveness of the proposed technique is also demonstrated through CAD simulations, showing a substantial reduction in input torque and joint reactions.

*Key-Words:* - fast-moving machinery, input torque, joint reactions, inertia forces, slider-crank mechanism, root-mean-square approximation.

Received: July 13, 2023. Revised: May 4, 2024. Accepted: June 13, 2024. Published: July 24, 2024.

## 1 Introduction

In the domain of industrial machinery, operating at high speeds has become imperative, with inertial forces taking precedence. The inertia inherent in moving links often results in significant fluctuations in a mechanism's input torque throughout its cycle. Given that motors are designed for peak operating conditions, mitigating these torque requirements holds economic appeal. Such mitigation not only allows for the use of less powerful motors but also contributes to reduced noise levels and enhanced longevity for select components, [1].

Devices for compensating inertia forces on input torque can be categorized into two main groups based on their installation location within the machine: *i*) Compensating cam systems installed at the machine's input element and unloading all transmissions from the motor to the input link; *ii*) Cyclic mechanism compensators with elastic connections directly engage the moving mass,

minimizing the fluctuations of the input torque and reactions on mechanism links. With the inclusion of a compensation device in the cyclic mechanism, surplus energy is stored and subsequently reintroduced into the mechanical system. Compensation devices utilized in this context include elements capable of accumulating and releasing potential or kinetic energy with minimal losses per cycle, such as springs, torsion rods, pneumatic and hydraulic devices, inertial systems, etc. Let us explore some studies dedicated to addressing this issue.

The reduction of input torque can be achieved through the optimal distribution of moving masses, [2], [3], [4], [5], [6], [7], [8], [9], [10]. Previous studies have focused on optimizing the mass parameters of moving links to achieve torque decrease. Additionally, researchers have explored another approach: the incorporation of springs into the mechanism for input torque compensation.

The synthesis of spring parameters proposed in [11] and [12] allows the minimization of input torque in planar mechanisms. Various methods for input torque compensation, such as incorporating cam sub-systems as discovered in [13], [14], [15], [16], [17], [18], have been investigated. This approach involves altering the input inertial parameters through prescribed cam profiles.

Additionally, alternative solutions involving articulated dyads and linkages, proposed in [19], [20], [21], [22] have been examined to minimize torque fluctuations. In these cases, optimal redistribution of moving masses to ensure torque compensation is achieved by attaching additional structural sub-systems to the original mechanism.

Flywheels driven by noncircular gears, as discussed in [23], [24], [25], [26] allow a means to completely balance the input torque. Nonlinear programming techniques have also been used to develop linkages with optimal dynamic properties, allowing the minimization of torque fluctuations [27], [28], [29].

Among the more efficient methods for input torque balancing is the creation of cam-spring mechanical systems, as detailed in [30], [31], [32], [33], [34], [35], [36], [37]. In such systems, the spring absorbs energy when torque demand is low and releases energy when demand is higher, providing precise compensation for load variations attributable to periodic torque. The synthesis and design of cam-spring mechanisms generally ensure complete compensation for periodic torque-induced load variations. Redundant drives have developed as a method for input torque compensation.

In [38], a servomotor was employed to achieve torque balancing in the linkage by varying the input speed function. Similarly, a redundant servomotor was utilized to address a similar challenge of simultaneous shaking moment and input torque balancing in four-bar linkages, as discussed in [39]. Furthermore, the combination of redundant drivers and gear trains has led to the proposal of various balancers for torque compensation in cyclic mechanisms, as presented in [40], and [41].

The study [42] addresses the problem of input torque compensation with the optimal connection of two identical slider-crank mechanisms (Figure 1).

In mechanical design, the challenge of balancing inertia forces on the frame and compensating for input torque are typically addressed as separate tasks. Traditionally, a mechanism can be balanced using well-known methods [10], and its input torque can then be compensated for using a complementary device.

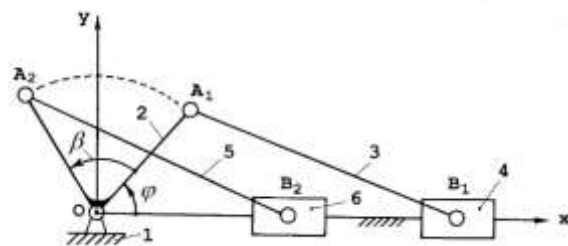


Fig. 1: Input torque compensation with the optimal connection of two identical slider-crank mechanisms, [42]

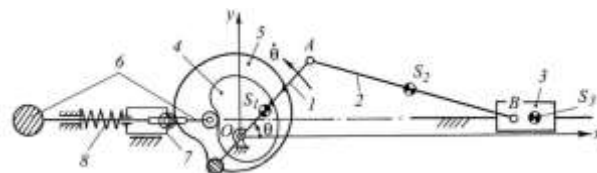


Fig. 2: Simultaneous inertia force balancing and torque compensation in slider-crank mechanisms, [10]

However, in the study [10], a novel design approach has been introduced, which advocates for simultaneous inertia force balancing and torque compensation in slider-crank mechanisms (Figure 2).

This paper deals with the inertia force compensation in high-speed mechanisms with reciprocating motion. It is carried out by providing two springs mounted between the slider and the frame, which compensate for the inertia force of the slider and, as a result, reduce the input torque and joint reactions of the mechanism.

## 2 Statement of the Problem

Figure 3 shows a slider-crank mechanism. The inertia force resulting from reciprocating motion can be expressed as a series:

$$F^{\text{int}} = -m\ddot{x} = mr[A_1(\dot{\varphi})^2 \cos\varphi + A_2mr(2\dot{\varphi})^2 \cos 2\varphi + A_4mr(4\dot{\varphi})^2 \cos 4\varphi + \dots] \quad (1)$$

with

$$A_1 = -1$$

$$A_2 = -\left(\frac{1}{4}\lambda + \frac{1}{16}\lambda^3 + \frac{5}{256}\lambda^5 + \dots\right)$$

$$A_4 = \frac{1}{16}\lambda^3 + \frac{15}{256}\lambda^5 + \dots$$

...

where,  $r = l_{OA}$  is the length of the crank,  $m$  is the mass associated with reciprocating motion,  $l = l_{AB}$

is the length of the coupler link,  $\lambda = r/l$ ,  $\varphi$  is the rotation angle of the crank and  $\dot{\varphi}$  = cont its angular velocity.

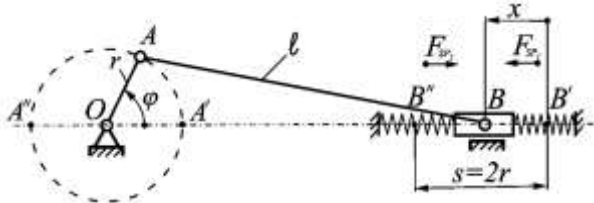


Fig. 3: Slider-crank mechanism with added springs

This series comprises an infinite number of terms, with each term denoting a simple harmonic motion characterized by a known frequency and amplitude. Higher-frequency amplitudes tend to be negligible, rendering only a small number of lower-frequency amplitudes significant. Considering the fourth or higher harmonics is seldom necessary.

Thus, the inertia force of the reciprocating motion can be expressed as:

$$F^{\text{int}} = -mr\dot{\varphi}^2(\cos\varphi + \lambda\cos 2\varphi) \quad (2)$$

taking into account that  $A_2 \cong -0.25\lambda$ .

In high-speed slider-crank mechanisms, this force is substantial, leading to increased input torque requirements and joint forces. The objective of this study is to introduce a solution aimed at minimizing the input torque and joint reactions. To achieve this goal, the slider-crank mechanism is equipped with two compression springs featuring linear characteristics, mounted between the slider and the frame. It is important to note that the stroke length is  $s=2r$ , and the additional springs generate the following extra forces:

$$F_{sp1} = k_1(s - x) \text{ and } F_{sp2} = k_2x \quad (3)$$

where,  $k_1$  and  $k_2$  are the stiffness coefficients of the springs.

In order to minimize the input torque and joint reactions due to the reciprocating inertia force, it is necessary to minimize:

$$F = F^{\text{int}} + k_1(s - x) - k_2x \rightarrow \min_{k_1, k_2} \quad (4)$$

Two solutions are considered below: on the base of the root mean square and maximum values minimization of function (4).

### 3 Minimization by Root Mean Square Value

For minimization of the root mean square (RMS) value

$$F_{RMS} = \sqrt{\int_0^{2\pi} (F(\varphi))^2 d\varphi / N} \rightarrow \min_{k_1, k_2} \quad (5)$$

it is necessary to minimize integral:

$$\int_0^{2\pi} (F(\varphi))^2 d\varphi = \int_0^{2\pi} (c_1 \cos \varphi + c_2 \cos 2\varphi + c_3)^2 d\varphi \rightarrow \min_{k_1, k_2} \quad (6)$$

where,

$$c_1 = r(k_1 + k_2) - mr\dot{\varphi}^2 \quad (7)$$

$$c_2 = -mr\lambda\dot{\varphi}^2 \quad (8)$$

$$c_3 = rk_1(1 - 0.25\lambda) - rk_2(1 + 0.25\lambda) \quad (9)$$

Hence, upon integration, the function that necessitates minimization is as follows:

$$\Delta_F = \pi(c_1^2 + c_2^2 + 2c_3^2) \rightarrow \min_{k_1, k_2} \quad (10)$$

To determine the minimum of the function  $\Delta_F$ , we impose the following conditions:

$$\frac{\partial \Delta_F}{\partial k_1} = 0, \quad \frac{\partial \Delta_F}{\partial k_2} = 0 \quad (11)$$

from which we obtain:

$$\begin{bmatrix} a_{11} & a_{12} \\ a_{21} & a_{22} \end{bmatrix} \begin{bmatrix} k_1 \\ k_2 \end{bmatrix} = \begin{bmatrix} A_1 \\ A_2 \end{bmatrix} \quad (12)$$

where,

$$a_{11} = r^2(0.125\lambda^2 - \lambda + 3) \quad (13)$$

$$a_{12} = a_{21} = r^2(0.125\lambda^2 - 1) \quad (14)$$

$$a_{22} = r^2(0.125\lambda^2 + \lambda + 3) \quad (15)$$

$$A_1 = A_2 = mr^2\dot{\varphi}^2 \quad (16)$$

Therefore, the stiffness coefficients of the springs are determined from equation (12):

$$k_1 = \begin{bmatrix} a_{11} & a_{12} \\ a_{21} & a_{22} \end{bmatrix}^{-1} \begin{bmatrix} A_1 & a_{12} \\ A_2 & a_{22} \end{bmatrix} \quad (17)$$

and

$$k_2 = \begin{bmatrix} a_{11} & a_{12} \\ a_{21} & a_{22} \end{bmatrix}^{-1} \begin{bmatrix} a_{11} & A_1 \\ a_{21} & A_2 \end{bmatrix} \quad (18)$$

#### 4 Minimization by Chebichev's Approximation

The quadratic approximation generally results in minor deviations on average from the given function. However, across various segments, the deviation can occasionally escalate to values significantly divergent from the average. The best function approximation is free from these flaws by introducing the minimum possible value of the maximum deviation from the given function:

$$\Delta_{\max} = \min \left\{ \max \left| F^{\text{int}} + k_1(s - x) - k_2x \right| \right\}.$$

According to Chebyshev's theorem on the best function approximation, it is necessary to find such polynomial coefficients (in the present study the stiffness coefficients of the springs  $k_1$  and  $k_2$ ) for which the maximum value of function (4) will be minimum, i.e.

$$\max \left| F^{\text{int}} + k_1(s - x) - k_2x \right| \rightarrow \min_{k_1, k_2} \quad (19)$$

In order to achieve such a minimization it is necessary and enough that the force  $F$  determined from (4) no less than  $n + 2$  ways reaches its limit values  $\pm \Delta_{\max}$  consecutively changing its sign in the interval  $[0, 2\pi]$ , i.e.

$$\begin{aligned} F^{\text{int}}(\varphi_i) + k_1(s - x(\varphi_i)) - k_2x(\varphi_i) \\ = \pm \Delta_{\max} \end{aligned} \quad (20)$$

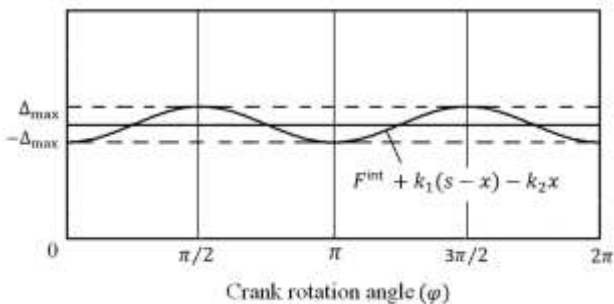


Fig. 4: Best function approximation

Given that for  $\varphi_i$ , the difference  $\Delta_{\max}$  should not exceed its limit value (Figure 4), its derivative at these points is reduced to zero, i.e. for half rotation of the input crank  $[0, \pi]$  is sufficient.

$$\frac{d(\Delta_{\max})}{d\varphi} = 0 \quad (i = 1, \dots, n) \quad (21)$$

Considering the extreme points, we obtain two additional equations, totaling  $n + 2$ . Please note that the function (4) is symmetrical and the minimization for half rotation of the input crank  $[0, \pi]$  is sufficient.

Thus, we obtain:

$$\begin{aligned} r \sin \varphi_i (m \dot{\varphi}_i^2 + 4 \lambda m \dot{\varphi}_i^2 \cos \varphi_i - k_1 - k_2) = \\ = 0 \end{aligned} \quad (22)$$

and we determine:

$$\sin \varphi_1 = \sin \varphi_3 = 0 \quad (23)$$

$$\cos \varphi_2 = (k_1 + k_2 - m \dot{\varphi}^2) (4 \lambda m \dot{\varphi}^2)^{-1} \quad (24)$$

However, taking into account that  $F(\varphi_1) = F(\varphi_3)$ , we obtain  $k_1 + k_2 = m \dot{\varphi}^2$  and consequently  $\varphi_2 = \pi/2$ .

By substituting the values of  $\varphi_1 = 0, \varphi_2 = \pi/2, \varphi_3 = \pi$  into equation (20), we obtain:

$$\begin{bmatrix} b_{11} & b_{12} & b_{13} \\ b_{21} & b_{22} & b_{23} \\ b_{31} & b_{32} & b_{33} \end{bmatrix} \begin{bmatrix} k_1 \\ k_2 \\ \Delta_{\max} \end{bmatrix} = \begin{bmatrix} B_1 \\ B_2 \\ B_3 \end{bmatrix} \quad (25)$$

where,

$$b_{11} = r(2 - 0.25\lambda) \quad (26)$$

$$b_{12} = 0.25\lambda r \quad (27)$$

$$b_{13} = -1 \quad (28)$$

$$b_{21} = r(1 - 0.25\lambda) \quad (29)$$

$$b_{22} = -r(1 + 0.25\lambda) \quad (30)$$

$$b_{23} = 1 \quad (31)$$

$$b_{31} = -0.25\lambda r \quad (32)$$

$$b_{32} = -r(2 + 0.25\lambda) \quad (33)$$

$$b_{33} = -1 \quad (34)$$

$$B_1 = mr \dot{\varphi}^2 (1 + \lambda) \quad (35)$$

$$B_2 = -mr \lambda \dot{\varphi}^2 \quad (36)$$

$$B_3 = -mr \dot{\varphi}^2 (1 - \lambda) \quad (37)$$

Therefore, the stiffness coefficients of the springs are as follows:

$$k_1 = \begin{bmatrix} b_{11} & b_{12} & b_{13} \\ b_{21} & b_{22} & b_{23} \\ b_{31} & b_{32} & b_{33} \end{bmatrix}^{-1} \begin{bmatrix} B_1 & b_{12} & b_{13} \\ B_2 & b_{22} & b_{23} \\ B_3 & b_{32} & b_{33} \end{bmatrix} \quad (38)$$

and

$$k_2 = \begin{bmatrix} b_{11} & b_{12} & b_{13} \\ b_{21} & b_{22} & b_{23} \\ b_{31} & b_{32} & b_{33} \end{bmatrix}^{-1} \begin{bmatrix} b_{11} & B_1 & b_{13} \\ b_{21} & B_2 & b_{23} \\ b_{31} & B_3 & b_{33} \end{bmatrix} \quad (39)$$

Considering that the angles  $\varphi_i$  already been determined and that the inertial force in the axial crank-slider mechanism are symmetric function, it is possible to obtain their more precise values of  $k_1$  and  $k_2$  by including their exact values in the equation (25).

Therefore, we derive the following equation:

$$\begin{bmatrix} s - x_{(\varphi=0)} & -x_{(\varphi=0)} & -1 \\ s - x_{(\varphi=\pi/2)} & -x_{(\varphi=\pi/2)} & 1 \\ s - x_{(\varphi=\pi)} & -x_{(\varphi=\pi)} & -1 \end{bmatrix} \begin{bmatrix} k_1 \\ k_2 \\ \Delta_{\max} \end{bmatrix} = \begin{bmatrix} -F_{(\varphi=0)}^{\text{int}} \\ -F_{(\varphi=\pi/2)}^{\text{int}} \\ -F_{(\varphi=\pi)}^{\text{int}} \end{bmatrix} \quad (40)$$

and determine

$$k_1 = \frac{\begin{bmatrix} -F_{(\varphi=0)}^{\text{int}} & -x_{(\varphi=0)} & -1 \\ -F_{(\varphi=\pi/2)}^{\text{int}} & -x_{(\varphi=\pi/2)} & 1 \\ -F_{(\varphi=\pi)}^{\text{int}} & -x_{(\varphi=\pi)} & -1 \end{bmatrix}}{\begin{bmatrix} s - x_{(\varphi=0)} & -x_{(\varphi=0)} & -1 \\ s - x_{(\varphi=\pi/2)} & -x_{(\varphi=\pi/2)} & 1 \\ s - x_{(\varphi=\pi)} & -x_{(\varphi=\pi)} & -1 \end{bmatrix}} \quad (41)$$

$$k_2 = \frac{\begin{bmatrix} -x_{(\varphi=0)} & -F_{(\varphi=0)}^{\text{int}} & -1 \\ -x_{(\varphi=\pi/2)} & -F_{(\varphi=\pi/2)}^{\text{int}} & 1 \\ -x_{(\varphi=\pi)} & -F_{(\varphi=\pi)}^{\text{int}} & -1 \end{bmatrix}}{\begin{bmatrix} s - x_{(\varphi=0)} & -x_{(\varphi=0)} & -1 \\ s - x_{(\varphi=\pi/2)} & -x_{(\varphi=\pi/2)} & 1 \\ s - x_{(\varphi=\pi)} & -x_{(\varphi=\pi)} & -1 \end{bmatrix}} \quad (42)$$

Let us illustrate the proposed method for unloading the input torque and reactions in joints

from variable inertia forces through a numerical example.

## 5 Illustrative Example with Simulation Results

Let us consider a slider-crank mechanism with following parameters:  $\dot{\varphi} = 100s^{-1}$ ,  $\lambda = 0.25$ ,  $m = 1.5\text{kg}$ ,  $r = 0.05\text{m}$ .

Firstly, root mean square minimization is considered.

The exact value of the reciprocating inertial force can be represented as follows **Σφάλμα! Το αρχείο προέλευσης της αναφοράς δεν βρέθηκε.**

$$F^{\text{int}} = -m\ddot{x} = -mr\dot{\varphi}^2 \left( \cos\varphi - \lambda \frac{\cos 2\varphi}{\cos \psi} - \frac{\lambda^3 \sin^2 2\varphi}{4 \cos^3 \psi} \right) \quad (43)$$

where,  $\psi = \sphericalangle ABO = \pi - \sin^{-1}(\lambda \sin \varphi)$ .

Then, from (13)-(16) we determine  $a_{11} = 0.0087\text{m}^2$ ,  $a_{12} = a_{21} = 0.0025\text{m}^2$ ,  $a_{12} = 0.0082\text{m}^2$ ,  $A_1 = A_2 = 37.5\text{Nm}$  and obtain the following values of the springs' stiffness coefficients:  $k_1 = 7972\text{N/m}$  and  $k_1 = 7004\text{N/m}$ . The root mean square minimization leads to the resulting force, which varies in the interval  $[-137.9\text{N}; 146.9\text{N}]$ .

Let us consider now the minimization by Chebichev's approximation. In this case, the expressions (41) and (42) have the following numerical values:

$$k_1 = \frac{\begin{bmatrix} 937.5 & 0 & -1 \\ -193.7 & -0.05635 & 1 \\ -562.5 & -0.1 & -1 \end{bmatrix}}{\begin{bmatrix} 0.1 & 0 & -1 \\ 0.04365 & -0.05635 & 1 \\ 0 & -0.1 & -1 \end{bmatrix}} \quad (44)$$

$$k_2 = \frac{\begin{bmatrix} 0.1 & 937.5 & -1 \\ 0.04365 & -193.7 & 1 \\ 0 & -562.5 & -1 \end{bmatrix}}{\begin{bmatrix} 0.1 & 0 & -1 \\ 0.04365 & -0.05635 & 1 \\ 0 & -0.1 & -1 \end{bmatrix}} \quad (45)$$

and the springs' stiffness coefficients:  $k_1 = 7942\text{N/m}$  and  $k_1 = 7055\text{N/m}$  with  $\Delta_{\max} = \pm 143\text{N}$ . Thus, the variation of reciprocating inertia force after minimization by Chebichev's approach becomes uniform, which varies in the interval  $[-143\text{N}; 143\text{N}]$ .

Figure 5 shows the variations of the reciprocating inertia force before compensation ( $F^{int}$ ), the compensation force developed by springs ( $F_{sp}$ ) and the resulting force after compensation ( $F$ ). It should be noted that the values of the resulting forces compensated by root mean square and maximum values are very close (the difference is no more than 5N) and they are shown by one graph in Figure 4. Obtained results show that the suggested compensation technique allows to reduce the maximum value of the reciprocating inertia force until 85%.

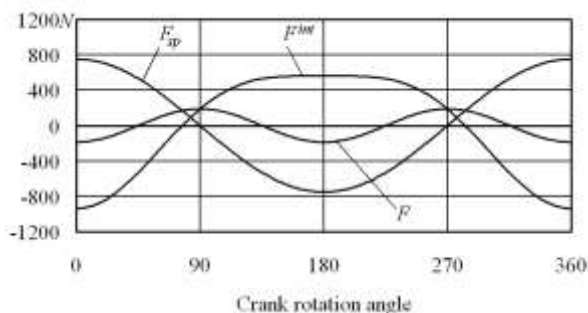


Fig. 5: Variations of reciprocating inertia force before compensation ( $F^{int}$ ), springs' elastic force ( $F_{sp}$ ) and the resulting force after compensation ( $F$ )

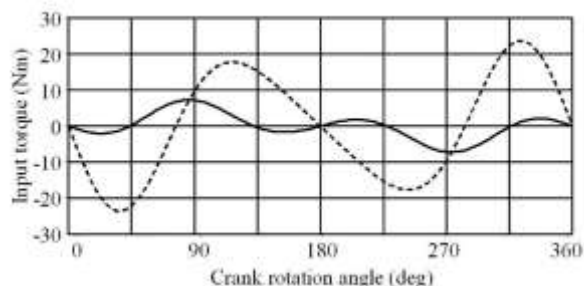


Fig. 6: Variations of the input torque

The examined mechanism has been simulated with the software ADAMS. Figure 6 presents the variations of the input torque before (dotted line) and after (full line) compensation. The numerical simulation showed that the reduction of the maximum values of the input torque is 71%.

Figure 7 presents the variations of the reaction in prismatic pair before (dotted line) and after (full line) compensation. In this case, the reduction of the maximum value of the joint reaction is 64%.

We also wish to highlight the versatility of the proposed compensation technique, which remains effective even in scenarios where external forces are exerted on the slider. These forces can be seamlessly incorporated into a function (4) through

analytical representation. It is important to note that the efficacy of compensation, as well as the optimal values for the stiffness coefficients of the springs, are contingent upon the specific characteristics of these external forces.

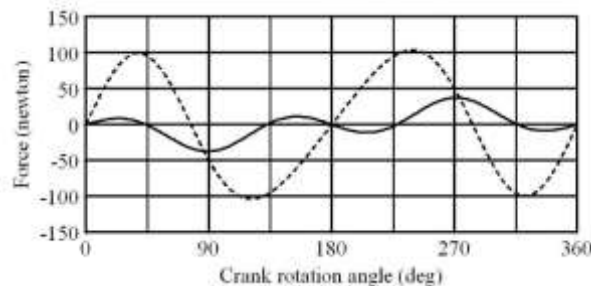


Fig. 7: Variations of the reaction in prismatic pair

However, it should be also noted that adding a spring between the slider and the frame in a crank-slider mechanism can have a significant impact on the system's resonance. This alters the stiffness and mass characteristics of the mechanical system, potentially shifting the system's natural frequency. If this new natural frequency approaches the frequency of external excitation, it can lead to amplification of oscillations and increase the risk of resonance. When external forces are applied to the mechanism, resonance can occur if the frequency of these external excitations corresponds to the system's natural frequency. This can result in significant oscillations, potentially leading to decreased performance. In such cases, to minimize the effects of resonance, it is essential to optimize the parameters of the springs calculated from inertia force compensation, based on the dynamic characteristics of the system and the anticipated operating conditions. This may require a thorough analysis of the system's dynamic behavior and experimental testing to validate the selected spring choices.

## 6 Conclusions

When a machine element having a large mass is given a reciprocating movement, the periodical variations in speed bring the variable dynamic loads, which on the one hand have several undesirable effects on the frame, as vibrations, on the other hand, they increase the joint reactions and require that great driving force must be applied.

In this paper, an arrangement for the compensation of inertia forces in the mechanisms with reciprocating moving links is proposed. It is shown that by a simple system containing two linear

compression springs, it is possible to minimize simultaneously the input torque and the joint reactions. It is important to note that the added elastic forces, which compensate for the alternative inertia forces are internal relative to the mechanical system, i.e. they do not perturb the shaking force and shaking moment balance of a mechanism. On the basis of an analytical approach, the conditions for the compensation are formulated by the minimization of the root-mean-square and maximum values of the inertia force of the reciprocating moving mass. The efficiency of the suggested technique is illustrated by the numerical example in which 71% of the input torque and 64% of the reaction in the prismatic pair are achieved.

It should be noted that previous works aimed at achieving a similar goal employed more complex design solutions, using additional mechanisms with cams and other similar elements. The advantages of this study include the simplicity of the compensating device's design and the fact that the solution is obtained purely analytically, significantly increasing the clarity of the solution and its ease of application in various engineering projects.

#### References:

- [1] B. Zappa, V. Lorenzo, P. Reghettini, R. Strada, Design of torque balancing mechanisms, *J. Mechanics Engineering and Automation*, vol. 7, pp. 312-320, 2017.
- [2] B.A. Hockey, An improved technique for reducing the fluctuation of kinetic energy in plane mechanisms. *J. Mechanisms*, vol. 6, pp. 405-418, 1971.
- [3] B.A. Hockey, The minimization of the fluctuation of input-shaft torque in planar mechanisms, *Mech. and Mach. Theory*, vol. 7, pp. 335-346, 1972.
- [4] J.L. Elliott, D. Tesar, The theory of torque, shaking force and shaking moment balancing of four link mechanisms, *Trans. ASME, J. Engineering for Industry*, Vol. 99B(3), pp. 715-721, 1977.
- [5] J.L. Elliott, D. Tesar, A general mass balancing method for complex planar mechanisms, *Mech. and Mach. Theory*, vol. 17(2), pp. 153-172, 1982
- [6] R.C. Soong, Minimization of the driving torque of full force balanced four-bar linkages. *J. Kao Yuan Institute of Technology*, pp. 591-594, 2001.
- [7] H.S. Yan, R.C. Soong, Kinematic and dynamic design of four-bar linkages by links counterweighing with variable input speed. *Mech. and Mach. Theory*, vol. 36(9), pp. 1051-1071, 2001.
- [8] V. Arakelian, Complete shaking force and shaking moment balancing of RSS'R spatial linkages, *J. Multi-body Dynamics*, Part K 221, pp. 303-310, 2007.
- [9] H. Chaudhary, Balancing of four-bar linkages using maximum recursive dynamic algorithm. *Mech. and Mach. Theory*, vol. 42, pp. 216-232, 2007.
- [10] V. Arakelian, S. Briot, *Balancing of linkages and robot manipulators. Advanced methods with illustrative examples*, Springer, Switzerland, 2015.
- [11] G.K. Matthew, D. Tesar, Synthesis of spring parameters to satisfy specified energy level in planar mechanisms, *ASME J. Engineering for Industry*, vol. 99B(2), pp. 341-346, 1977.
- [12] V. Arakelian, J.-P. Le Baron, M. Mkrtchyan, Design of Scotch yoke mechanisms with improved driving dynamics, *J. Multi-body Dynamics*, vol. 230(4), pp. 379-386, 2016.
- [13] B. Demeulenaere, J. Swevers, J. De Schutter, Input torque balancing using a cam-based centrifugal pendulum: design procedure and example, *J. Sound Vib.*, vol. 283 (1-2), pp. 1-20, 2005.
- [14] B. Demeulenaere, J. Swevers, J. De Schutter, Input torque balancing using a cam-based centrifugal pendulum: design optimization and robustness, *J. Sound Vib.*, vol. 283 (1-2), pp. 21-46, 2005.
- [15] B. Demeulenaere, J. De Schutter, Input torque balancing using inverted cam mechanisms, *ASME J. Mech. Design*, vol. 127(6), pp. 887-900, 2005.
- [16] B. Demeulenaere, P. Spaepen, S. Masselis et al, Experimental validation of input torque balancing applied to weaving machinery, *ASME J. Mech. Design.*, vol. 130 (2), Paper 022307(1-10), 2008.
- [17] T.M. Lee, D.Y.Lee, H.C. Lee, M.Y. Yang, Design of cam-type transfer unit assisted with conjugate cam and torque control cam, *Mech. and Mach. Theory*, vol. 44(6), pp. 1144-1155, 2009.
- [18] F. Gao, Y. Liu, W.-H. Liao, Cam profile generation for cam-spring mechanism with desired torque. *Journal of Mechanisms and Robotics*, vol. 10, Paper 041009, 2018.
- [19] P. Kulitzscher, Power compensation of coupling gears by changing the mass distribution or additional coupling gears, mechanical engineering (Leistungsausgleich von koppelgetrieben durch veränderung der

- massenverteilung oder zusatzkoppelgetriebe), *Maschinenbautechnik*, vol. 19, pp. 562–568, 1970.
- [20] C. Bagci, Synthesis of the plane four-bar mechanism for torque generation, and application to a case study for the design of a new balancing mechanism for rotary top brush in power wax car washing machines, *ASME Mechanisms Conference*, Paper No. 78-DET-71, 1978.
- [21] Z. Huang, Synthesis of a dyad to balance the inertia input torque of crank, rocker mechanisms, In: *Proceeding of 4th International conference on the Theory of Machines and Mechanisms Symposium on Linkage and CAD Methods*, Romania, Vol. I-1, 1985, pp. 185-192.
- [22] L. D. Yong, Z. Huang, Input torque balancing of linkages, *Mech. Mach. Theory*, vol. 24, pp. 99–103, 1989.
- [23] I.S. Kochev, General method for active balancing of combined shaking moment and torque fluctuations in planar linkages, *Mech. Mach. Theory*, vol. 25, pp. 679–687, 1990.
- [24] D. B. Dooner, Use of noncircular gears to reduce torque and speed fluctuations in rotating shafts,” *ASME J. Mech. Des.*, vol. 119, pp. 299–306, 1997.
- [25] D. Barkah, B. Shafiq, D. Dooner, 3D mesh generation for static stress determination in spiral noncircular gears used for torque balancing, *ASME J. Mech. Des.*, vol. 124, pp. 313–319, 2002.
- [26] Yao, Y.A., Yan, H.S., A new method for torque balancing of planar linkages using non-circular gears. *Journal of Mechanical Engineering Science Part C*, vol. 217(5), pp. 495-503, 2003.
- [27] H. Dresig, S. Schönfeld, Computer-aided optimization of drive and frame force sizes of planar coupling gears (Rechnergestützte Optimierung der Antriebs- und Gestellkraftgrößen ebener Koppelgetriebe Teil I), *Mech. and Mach. Theory*, vol. 11(6), pp. 363-370, 1976.
- [28] T.W. Lee, C. Cheng, Optimum balancing of combined shaking force, shaking moment, and torque fluctuations in high speed linkages, *ASME J. Mech. Transm. Autom. Des.*, Vol. 106 (2), pp.242–251, 1984.
- [29] H. Chaudhary, S.K. Saha, An optimization technique for the balancing of spatial mechanisms, *Mech. and Mach. Theory*, vol. 43(4), pp. 506-522, 2008.
- [30] M. Arakawa, M. Nishioka, N. Morita, Torque compensation cam mechanism. In: *Proc. Joint International Conf. on Advanced Science and Technology*, Zhejiang University, Hangzhou, China, pp. 302-305, 1997.
- [31] M. Nishioka, M. Yoshizawa, Direct torque compensation cam mechanisms, *Transactions of the Japan Society of Mechanical Engineers*, 61(585), pp. 2020-2024, 1995.
- [32] M. Nishioka, Design of torque compensation cam using measured torque distribution, In: *Proceedings of the 10th World Congress on the Theory of Machines and Mechanisms*, Finland, 1999), pp. 1471-1476.
- [33] C.E. Benedict, G.K. Matthew, D. Tesar, Torque balancing of machines by sub-unit cam systems. In: *Proceedings of the 2nd Applied Mechanism Conference*, paper No. 15, Oklahoma State University, Stillwater, Oklahoma, 1971.
- [34] W. Funk, J. Han, on the complete balancing of the inertia-caused input torque for plane mechanisms. In: *Proceedings of the Design Engineering Technical conference*, Irvine, California, 1996.
- [35] T. Guilan, F. Haibo, Z. Weiyi, A new method of torque compensation for high speed indexing cam mechanisms, *ASME Journal of Mechanical Design*, vol. 121, pp. 319-323, 1999.
- [36] C.-J. Wu, J. Angeles, The optimum synthesis of an elastic torque-compensating cam mechanism. *Mech. and Mach. Theory*, vol. 36 (2), pp. 245-259, 2001.
- [37] D.-Y. Lin, B.-J. Hou, C.-C. Lan, A balancing cam mechanism for minimizing the torque fluctuation of engine camshafts, *Mech. and Mach. Theory*, vol. 108, pp. 160–175, 2017.
- [38] Y.A. Yao, H.S. Yan, H.J. Zou, Dynamic design of variable speed planar linkages, *Chinese Journal of Mechanical Engineering*, vol. 18(1), pp. 51-54, 2005.
- [39] Z. Sun, B. Zhang, J. Huang, W.J. Zhang, on a mechatronics approach to balancing of robotic mechanisms: redundant servo motor, in: *Proceedings of the 5th International Conference on the Advanced Mechatronics*, October 4-6, Osaka, Japan, 2010, pp. 675-680.
- [40] J. Sun, Y. Yao, Integrated design of an active torque balancing mechanism and a planetary gear reducer, *J. System Design and Dynamics*, (No. 10-0074), pp. 391-405, 2010.
- [41] J. Sun, Y. Yao, An active gear balancer for torque compensation, *ASME J. Mech. Design*, vol. 133, Paper 014502/ 01-10, 2011.



- [42] V. Arakelian, Design of torque-compensated mechanical systems with two connected identical slider-crank mechanisms. *J. Mechanisms and Robotics*. vol. 14(2), paper 024503, 2022

**Contribution of Individual Authors to the Creation of a Scientific Article (Ghostwriting Policy)**

The author contributed in the present research, at all stages from the formulation of the problem to the final findings and solution.

**Sources of Funding for Research Presented in a Scientific Article or Scientific Article Itself**

No funding was received for conducting this study.

**Conflict of Interest**

The author has no conflict of interest to declare.

**Creative Commons Attribution License 4.0 (Attribution 4.0 International, CC BY 4.0)**

This article is published under the terms of the Creative Commons Attribution License 4.0

[https://creativecommons.org/licenses/by/4.0/deed.en\\_US](https://creativecommons.org/licenses/by/4.0/deed.en_US)